Seepage forces, important factors in the formation of horizontal hydraulic fractures and bedding-parallel fibrous veins ('beef' and 'cone-in-cone')

P.R. Cobbold, N. Rodrigues

To cite this version:

P.R. Cobbold, N. Rodrigues. Seepage forces, important factors in the formation of horizontal hydraulic fractures and bedding-parallel fibrous veins ('beef' and 'cone-in-cone'). Geofluids, 2007, 7 (3), pp.313-322. 10.1111/j.1468-8123.2007.00183.x . insu-00180021

Seepage forces, important factors in the formation of horizontal hydraulic fractures and bedding-parallel fibrous veins ("beef" and "cone-in-cone")

Peter R. Cobbold and Nuno Rodrigues

Géosciences-Rennes (UMR6118), CNRS et Université de Rennes 1, Campus de Beaulieu, 35042 Rennes Cedex, France

Principal author: peter.cobbold@univ-rennes1.fr

Suggested running title: Seepage forces and "beef"

Abstract

Bedding-parallel fibrous veins ("beef" and "cone-in-cone") are common to a number of sedimentary basins, especially those containing black shale. The type locality is SW England. The commonest mineral in the fibres is calcite. The fibres indicate vertical opening, against the force of gravity. In the past, this has been attributed to fluid overpressure. However, a simple analysis, based on Von Terzaghi's concepts, leads to the conclusion that, for the fractures to be horizontal, either the rock must be anisotropic, or it must be subject to horizontal compression. By means of a more complete analysis, supported by physical models, we show that horizontal fractures are to be expected, even if the rock is isotropic and there are no tectonic stresses. Upward fluid flow, in response to an overpressure gradient, imparts seepage forces to all elements of the solid framework. The seepage forces counteract the weight of the rock, and even surpass it, generating a tensile effective stress. The process may lead, either to tensile hydraulic fracturing, or to dilatant shear failure. We suggest that

these two failure modes, and the availability of suitable solutes, explain the frequent occurrence of “beef” and “cone-in-cone”, respectively.

Introduction: bedding-parallel veins (“beef” and “cone-in-cone”)

Bedding-parallel veins of fibrous calcite or other minerals are common to a number of sedimentary basins, especially those containing black shale. Good examples are the veins of fibrous calcite in Jurassic strata along the coastal cliffs of SW England (Fig. 1). In the 1800s, quarrymen called this material “beef”, because of its resemblance to fibrous steak. So common is this material that it has given its name to a stratigraphical unit, the “Shales-with-Beef” of Liassic age (Lang et al., 1923). On average, the veins appear to have grown in a horizontal attitude and the fibres appear to have grown vertically. Less common in the area are “cone-in-cone” structures: multiply nested cones of fibrous calcite, in which the fibres have also grown vertically on average.

In the early days of geological investigation, beef and cone-in-cone attracted attention and were subjects of debate (Sorby, 1860). Were the structures “displacive”, in the sense of the walls moving apart (the modern term would be “dilatant”)? What was the nature of the forces involved? Did the fibres passively infill fracture space, or did they actively push the host rock apart by force of crystallization? These questions found no immediate answers and they are still relevant today (Hilgers and Urai, 2005; Wiltschko and Morse, 2001).

From studies of fibrous veins, especially those containing oblique fibres, there is a consensus that the fibres grow incrementally, partly or totally tracking the history of relative displacement of the walls (Taber, 1918; Durney and Ramsay, 1973). In some examples, opening and infilling seem to have occurred episodically, by a crack-seal mechanism

(Ramsay, 1980). In other examples, there may have been no loss of continuity within the fibres, as they grew.

Although calcite is perhaps the commonest fibrous mineral in dilatant veins, other infilling minerals may also adopt a fibrous habit. Examples are gypsum (Shearman et al., 1972; Hilgers and Urai, 2005), quartz (Ramsay, 1980; Hilgers and Urai, 2005), pyrobitumen or carbon (Parnell, 1999), dolomite, halite, strontianite, celestite, various borates such as ulexite, barite, the various kinds of asbestos, albite, emerald, and even precious metals, such as gold and silver. Arguably, almost any mineral may adopt a fibrous habit, if it grows during progressive or episodic opening of a vein, especially within porous rock. However, some species are undoubtedly more common than others. Intuitively, cryptocrystalline materials, such as pyrobitumen and some metals, are less likely to be truly fibrous. We suggest that the name “beef” should not be restricted to veins of calcite, but should encompass all fibrous bedding-parallel veins, regardless of their composition. In what follows, we will use the term in this sense.

Our current understanding is that fibrous minerals grow by precipitation, mainly from supersaturated aqueous solutions, as a result of chemical reactions, or changes in physical conditions, especially temperature and pressure. Several experimenters have succeeded in reproducing fibrous textures by precipitation and growth of crystals from supersaturated solutions, either into open space (Taber, 1918), or into a crack (Means and Li, 2001; Hilgers and Urai, 2002; Nollet et al., 2006). However none of these experiments have provided insights into the mechanics of fracturing, because the cracks were artificial and the specimens were too thin to allow adequate monitoring of stresses.

One possibility is that fracturing is due to relatively high pressures of fluid circulating through the pores.

Fluid overpressure and fluid flow

High values of pore fluid pressure are common in sedimentary basins, especially at depth (Swarbrick et al., 2002). Commonly, the fluid pressure increases with depth, but there may be significant deviations from such a simple trend. If the pressure is greater than that predicted by the weight of an equivalent column of water, it is said to be an overpressure.

The frequent occurrence of fluid overpressure in sedimentary basins has led to an intense debate concerning its origin. Amongst the many possible causes, the most popular would seem to be mechanical compaction, hydrocarbon generation, or a combination of both (Swarbrick et al., 2002). As shale compacts readily and may also generate hydrocarbons upon burial, it is perhaps no accident that beef is common in such rock. In this context, it is intriguing that some beef contains solid hydrocarbons between calcite fibres, or liquid hydrocarbons within them. Examples have been described from Jurassic source rocks in the Neuquén Basin of Argentina (Parnell and Carey, 1995; Parnell et al., 2000). Horizontal fractures infilled with bitumen alone have been described from several areas, including the Neuquén Basin (Parnell and Carey, 1995) and New York State (Lash and Engelder, 2005). Fractures that carry hydrocarbons, including beef, may provide valuable evidence for hydrocarbon generation as a contributing cause of overpressure.

Darcy’s Law of steady fluid flow in a permeable medium provides an explanation for pressure profiles of simple form (Fig. 2; Appendix). The law states that the rate of flow in a given direction is proportional to the permeability and to the overpressure gradient. Consider three examples.

1. A linear pressure profile is an indication that permeability is invariant with depth (Fig. 2A).

2. A local pressure ramp will occur across a sealing layer of relatively small permeability (Fig. 2B). The fluid pressure then reaches a maximum at the base of the sealing layer.
3. A parabolic hump is an indication that fluid is being generated within a source layer of small permeability (Fig. 2C). The fluid pressure then reaches a maximum about half way up the layer, instead of at its base.

In the last two examples, the fluid pressure may locally attain or even surpass lithostatic values.

Hydraulic fracturing

A major impetus for understanding the macroscopic mechanisms of beef formation came from the petroleum industry, when hydraulic fracturing was found to be the reason for borehole break-outs (Hubbert and Willis, 1957). A dilatant fracture propagates readily through brittle rock, if it contains a mobile fluid under high pressure, such as drilling mud. Break-outs occur if the fluid pressure exceeds the sum of (1) the compressive stress in the host rock, acting normal to the fracture, and (2) the tensile strength of the rock.

It is useful to distinguish between two mechanisms of hydraulic fracturing (Mandl and Harkness, 1987). In external hydraulic fracturing, a fluid coming from outside penetrates an impermeable rock. This mechanism is generally held to be responsible for magmatic dykes and sills. In internal hydraulic fracturing, an overpressured fluid migrates through pore space, generating a fracture at an internal point of weakness. This mechanism is held to be responsible for mineral-filled veins.

Hydraulic fracturing due to overpressure has been seen as a potential mechanism for opening bedding-parallel veins (Hillier and Cosgrove, 2002; Shearman et al., 1972; Stoneley, 1983).

Effective stresses and seepage forces

On considering a permeable material, it is useful to distinguish between (1) the total stress, acting on both the solid framework and the pore fluid, and (2) the effective stress, acting on the solid framework alone. These concepts originated in soil mechanics (Von Terzaghi, 1923). To our knowledge, they were first used in geology to explain ready sliding on a flat-lying thrust, as a result of fluid overpressure (Hubbert and Rubey, 1959). On applying the concepts to an isotropic rock, one finds that a horizontal fracture can form, only if the least effective stress is vertical, and the fluid overpressure exceeds the weight of the overburden by an amount equal to the tensile strength of the solid framework. However, in a purely lithostatic situation, where a sedimentary basin is subject to no forces except those of gravity, the greatest effective stress should be vertical and the least effective stress should be horizontal (Sibson, 2003). On this basis, beef should not form in lithostatic basins containing isotropic rock. On the contrary, necessary conditions for the formation of beef would seem to be, either (1) a context of horizontal compression, due to additional tectonic forces, or (2) a high susceptibility to fracturing along bedding, in other words, an anisotropy of tensile strength (Cosgrove, 1995, 2001; Lash and Engelder, 2005).

Recently it has been argued (and demonstrated by physical modelling) that although von Terzaghi's concept would appear to be correct, it is dangerous to calculate the effective stress at a point, by first considering the total stress without regard for fluid flow, and then subtracting the fluid overpressure (Cobbold et al., 2001; Mourgues and Cobbold, 2003). This is because overpressure tends to vary in space, so that a pore fluid migrates in response to its gradient, according to Darcy's Law. Microscopically, the migrating fluid imparts a seepage force to each element of the solid framework and this seepage force modifies the balance of forces acting on the element. Macroscopically, the seepage force per unit volume is equal to the overpressure gradient (see Mourgues and Cobbold, 2003, for a more detailed discussion of this topic). A complete analysis should therefore take seepage forces into account. On doing so, one finds that, although the greatest effective stress in most sedimentary basins should be vertical, as indeed it is according to measurements on many wells (Hillis, 2003), in extreme situations the greatest effective stress may become horizontal, as a result of seepage forces, and this will be the subject of our analysis.

Horizontal hydraulic fractures in physical models

Horizontal hydraulic fractures have been reported in a number of experiments on physical models.

For example, in experiments on fluid escape structures, in which overpressured water flowed upward through horizontal layers of fine-grained glass spheres and silicon carbide, horizontal water-filled fractures appeared beneath the least permeable layers (Nichols et al., 1994, their fig. 3).

In other experiments, the tensile strengths of homogeneous cohesive powders (organic polymers) have been measured experimentally, by forcing gas upward through columns of particles (Valverde et al., 1998; Watson et al., 2001). The experimenters reported that horizontal cracks formed, when the fluid overpressure exceeded the weight of the overburden.

We have done similar tests, to determine the physical properties of silica powder, for a grain size between 75 and 125 μm. Such a powder typically is cohesive and has a small tensile strength, enabling it to form open fractures (Galland et al., 2006). The apparatus was a cylindrical shear box, 11 cm in diameter, similar to the one of Mourgues and Cobbold (2003). After having been poured into the apparatus, the density of the powder was approximately 1.4 g cm^{-3}. The pore fluid was compressed air. The fluid pressure was measured at a number of regularly spaced points within the powder, by means of hypodermic needles, connected to U-tubes filled with water. The vertical fluid pressure profile was very close to linear, according to Darcy's Law, and the calculated permeability was 2.8 darcy. When the air flowed upwards, the apparent weight of the powder decreased, presumably as a result of seepage forces. The highest pressure that the powder was able to sustain was slightly larger than its weight, but we lack precision on this critical value of pressure, because of difficulties in correcting for sidewall friction (see Mourgues and Cobbold, 2003).

As the fluid pressure increased, internal structures appeared in the following four stages.

1. Small horizontal cracks formed within the powder. The cracks connected to small gas chimneys near the upper surface (Fig. 3).
2. The cracks coalesced, to form large jagged horizontal fractures. These fractures then widened, filling with air, and the overburden lifted.
3. The fluid pressure dropped suddenly and the fractures became unstable, migrating upward.
4. When the fractures reached the surface, the powder started to bubble.

Further tests will be necessary to explain this sequence of events. For the purposes of this paper, we note that horizontal hydraulic fractures formed when the fluid pressure exceeded the weight of overburden. The experiments therefore provide a physical basis for the analysis that follows.

Mechanical analysis

In this section, we develop the equations for elastic deformation and brittle failure of a sedimentary column, which is subject to gravity and seepage forces (Fig. 4). We assume a lithostatic context, in which the column is laterally confined, so that there are no horizontal strains. The effect of gravity (weight of overburden) is to generate a compressive stress that increases with depth. The effect of vertical seepage forces (overpressure gradient) is to counteract the weight, or even to overcome it. The aim of the analysis is to determine the conditions under which a horizontal dilatant fracture may develop.

Equations of linear elasticity

During progressive loading, most rocks undergo a first phase of small but recoverable elastic deformation, before reaching a yield point (Jaeger and Cook, 1979). Subsequent deformation is mainly non-elastic and irrecoverable. We consider each of these phases in turn.

For the elastic phase, the relationship between applied stress and infinitesimal strain is approximately linear. For simplicity, let us therefore assume linear isotropic elastic behaviour, as expressed by the following equations in three dimensions (Jaeger and Cook, 1979, page 110):

$$\begin{aligned}\sigma_1 &= (\lambda + 2G)\varepsilon_1 + \lambda\varepsilon_2 + \lambda\varepsilon_3\\ \sigma_2 &= \lambda\varepsilon_1 + (\lambda + 2G)\varepsilon_2 + \lambda\varepsilon_3\\ \sigma_3 &= \lambda\varepsilon_1 + \lambda\varepsilon_2 + (\lambda + 2G)\varepsilon_3\end{aligned} \quad (1)$$

Here σ_1, σ_2 and σ_3 are principal stresses (positive, when compressive); $\varepsilon_1, \varepsilon_2$ and ε_3 are principal infinitesimal strains (positive, when shortening); and λ and G are elastic constants (Lamé parameters). Notice that the composite factor $(\lambda + 2G)$ relates stress and strain in one and the same direction, whereas λ relates stress and strain in two perpendicular directions.

Lithostatic setting

In a sedimentary basin that is not subject to tectonic loading, internal stresses are mainly due to gravity. Consider such a lithostatic setting. Assume that there are no horizontal strains, only a vertical compaction $(\varepsilon_1 \neq 0, \varepsilon_2 = \varepsilon_3 = 0)$. The greatest stress is vertical. The least stresses are horizontal and equal in all directions, so that $\sigma_2 = \sigma_3$. Under these conditions of axial symmetry, equations (1) simplify to (Jaeger and Cook, 1979, page 113):

$$\begin{aligned}\sigma_1 &= (\lambda + 2G)\varepsilon_1\\ \sigma_2 &= \lambda\varepsilon_1\\ \sigma_3 &= \lambda\varepsilon_1\end{aligned} \quad (2)$$

Hence:

$$\sigma_2 = \sigma_3 = \left(\frac{\nu}{1-\nu}\right)\sigma_1 \quad (3)$$

where $\nu = \dfrac{\lambda}{2(\lambda + G)}$ is Poisson's ratio.

Equation (3) is a linear relationship between the greatest and least principal stresses, of the form $\sigma_3 = k_e\sigma_1$, where k_e is an elastic constant of proportionality. For most rocks, ν is between 1/4 and 1/3 (Jaeger and Cook, 1979), so that k_e is between 0.33 and 0.5.

If the rock yields, the equations of linear elasticity no longer hold. Instead, the stresses satisfy a yield criterion. Simplest is the linear relationship of Coulomb for a frictional but non-cohesive material:

$$\tau = \mu\sigma_n \tag{4}$$

Here τ and σ_n are the shear stress and normal stress acting on a plane, and μ is a constant, the coefficient of internal friction. In a space of shear stress versus normal stress (Mohr space, Fig. 5), equation (4) plots as a straight line through the origin (a linear Mohr envelope) and the state of stress plots as a circle (the Mohr circle). Shear failure (Coulomb slip) occurs if the circle touches the straight line.

By simple trigonometry (Fig. 4),

$$\sin\phi = (\sigma_1 - \sigma_3)/(\sigma_1 + \sigma_3) \tag{5}$$

Hence:

$$\sigma_3 = \left(\frac{1-\sin\phi}{1+\sin\phi}\right)\sigma_1 \tag{6}$$

Here ϕ is the angle of internal friction of the material, so that $\mu = \tan\phi$. Equation (6) is another linear relationship between greatest and least stresses, of the form $\sigma_3 = k_y\sigma_1$, this time for yield. For most granular materials and brittle rock, ϕ is between 30º (Byerlee, 1978) and 50º (Mourgues and Cobbold, 2003). Therefore k_y is between 0.13 and 0.33.

On comparing the elastic and brittle behaviours, we see that for most rocks, $k_e \leq k_y$. This means that the failure envelope is steeper than the elastic envelope (Fig. 6). Hence the rock does not yield under lithostatic conditions, except at the origin, where all stresses vanish, this being a trivial solution.

Fluid flow through a non-cohesive material in a lithostatic setting

Now consider that a pore fluid is flowing upward, as a result of a vertical gradient in pressure that is greater than hydrostatic, in other words, an overpressure gradient. According to the principle of Von Terzaghi (1923), the overpressure takes up part of the load, reducing the effective stress in the solid framework, so that:

$$\sigma_1' = \sigma_1 - P$$
$$\sigma_3' = \sigma_3 - P \qquad (7)$$

Here P is the overpressure and σ_1' and σ_3' are the greatest and least values of effective stress in the solid framework. If we assume that fluid flow has no effect other than this, the Mohr circle displaces toward the origin by an amount equal to *P,* without any change in size (Fig. 7). This simple result can be found in many well-known geological publications, including articles (Hubbert and Rubey, 1959; Sibson, 2003) and textbooks (e.g. Jaeger and Cook, 1979; Price and Cosgrove, 1990). However, it may be dangerously oversimplified, for situations in which there is fluid flow (Mourgues and Cobbold, 2003). Darcy's Law for fluid flow implies that seepage forces act on each solid element of the framework. The seepage forces modify the general balance of forces on the element. For upward flow, the seepage forces act vertically, not horizontally. Hence the vertically integrated effective stress will be reduced by an amount equal to the vertically integrated overpressure:

$$\sigma_1^{'} = \sigma_1 - P \tag{8}$$

However, the same is not true for the horizontal direction, in which there are no seepage forces. Instead, for elastic deformation in non-cohesive material under lithostatic conditions, the horizontal effective stress should be directly proportional to the vertical effective stress (Hillis, 2003):

$$\sigma_3^{'} = k_e \sigma_1^{'} = k_e \left(\sigma_1 - P\right) \tag{9}$$

It is convenient to express the overpressure P as a fraction of the total vertical stress:

$$P = \lambda \sigma_1 \tag{10}$$

Substituting (10) in (9):

$$\sigma_3^{'} = k_e (1 - \lambda) \sigma_1 \tag{11}$$

This relationship provides a good measure of the way in which horizontal stresses vary with depth in many overpressured basins (Hillis, 2003). As the overpressure increases, the Mohr circle not only shifts to the left in Mohr space, but also decreases in size (Fig. 8; Hillis, 2003; Mourgues and Cobbold, 2003). Eventually, at the origin, the Mohr circle reduces to a point.

Only at that point does the circle touch the failure envelope. All other situations are stable. Thus our analysis cannot account for the formation of bedding-parallel veins in a lithostatic setting, even if there is fluid flow. Some other factor is required. In any case, for a material to undergo tensile failure, it must have a tensile strength. Let us therefore incorporate this factor.

Fluid flow through cohesive material in a lithostatic setting

For rocks also that have tensile strength, the failure envelope in Mohr space enters the field of tensile stress, and in general it curves as it does so (Fig. 9). The intercept of the failure envelope on the vertical axis is the cohesion; and the intercept on the horizontal axis is the tensile strength.

In such a cohesive material, the fluid overpressure may become greater than the weight of overburden. The seepage force provides a lift. The weight compensates for part of it. The remainder causes a tensile stress and consequent elastic stretching. As the overpressure increases, the Mohr circles for effective stress become progressively larger, but this time in the tensile field. The least stress is now in absolute tension and it acts vertically. It is proportional to the greatest stress, according to the relationship $-\sigma_3^{'} = -k_y\sigma_1^{'}$. Thus the greatest stress is also tensile, but it acts horizontally.

Eventually, the Mohr circle may touch the failure envelope. If it does so at a point on the horizontal axis, the rock will fail in tension, producing a horizontal open fracture. For this to happen, the tensile strength should be smaller than the cohesion. Under these conditions, the fluid overpressure is equal to the overburden weight plus the tensile strength. This provides a simple and rather general explanation for the origin of beef.

Alternatively, if the Mohr circle touches the failure envelope at points above or below the horizontal axis, the rock will fail in mixed mode (shear and dilation), producing a conical fracture. For this to happen, the cohesion should be smaller than the tensile strength. This result may explain the origin of some cone-in-cone structures.

Discussion

According to the above analysis, large vertical seepage forces may cause the principal effective stresses to become tensile. Because the least effective stress is vertical, fractures may form in horizontal orientations. This result is simple and quite general, in the sense that it does not appeal to any particular tectonic setting. On the contrary, it assumes that stresses are lithostatic and that vertical forces are due to gravity and fluid flow. According to this analysis, it should be no surprise to find beef in sedimentary basins, even if the rock is isotropic and tectonic stresses are negligible.

If tectonic stresses do come into play, then their effects will add to those of seepage forces. Thus one would expect to find beef in a compressional setting. In contrast, in an extensional or strike-slip setting, where the least effective stress is horizontal, one would expect to find vertical veins.

The beef in the Liassic shale of SW England is parallel to bedding. If it formed in a horizontal attitude during early burial, when the tectonic context of the Wessex Basin was extensional (Underhill and Stoneley, 2003), this could mean that seepage forces were more significant than tectonic forces. Alternatively, the beef may have formed in a later context of Cretaceous or Tertiary compression, when the Wessex Basin became inverted. Clearly it would be of great interest to be able to date the formation of this beef – and of other beef in general.

To summarize this section, strong overpressure is capable of generating seepage forces as large as, or larger than, the weight of overburden. Thus seepage forces should not be neglected in mechanical analyses of failure.

Conclusions

By considering elastic behaviour, followed by yield, we have shown that bedding-parallel veins of fibrous calcite or other minerals (beef and cone-in-cone) may form in an isotropic rock, under lithostatic conditions, if there is enough overpressure. This result cannot be obtained from Von Terzaghi's concept of effective stress in its simplest form, as carried by most geological textbooks and articles. Instead, it is necessary to invoke seepage forces, which inevitably exist during Darcy flow. The vertical seepage forces that accompany upward flow, in response to an overpressure gradient, counteract the weight of overburden and may even surpass it, generating a vertical tensile stress in the solid framework. If horizontal seepage forces are negligible, the value of the horizontal effective stress results only from the elastic proportionality between principal stresses. Thus the horizontal stress is also tensile. However, it is smaller in magnitude than the vertical stress. If the rock fails in tension, the fractures will therefore be horizontal. This provides a simple but universal explanation for the occurrence of beef in tectonically inactive settings. If the rock fails in shear, the fractures will be conical and dilatant. This may provide an explanation for cone-in-cone structures.

Experiments on cohesive granular materials, under lithostatic conditions, where the only forces are due to gravity and overpressure, bear out the theoretical predictions.

The above results may change if there are additional stresses of tectonic origin. Beef is to be expected in a compressional context, less so in an extensional or strike-slip context. Beef is also more likely to occur if the rock is mechanically anisotropic, or has internal surfaces of weakness in tension.

Acknowledgments

Nuno Rodrigues thanks the "Fundação para a Ciência e Tecnologia", Portugal, for a post-graduate studentship (number SFRH / BD / 12499 / 2003). We thank Dr Ian West of Southampton Univeristy for showing us some of the best exposures of beef in SW England.

Appendix. Steady vertical flow of a pore fluid

In this Appendix, we derive the equations for pressure profiles due to steady Darcy flow of a pore fluid in a vertical direction, including a source term.

In one (vertical) dimension, Darcy's Law for steady fluid flow through a porous medium takes the form:

$$q = - (k/\mu) (dp/dz - \rho g) \quad \text{(A1)}$$

Here q is the macroscopic rate of vertical flow or Darcy velocity (positive downwards), k is the intrinsic permeability, μ is the viscosity of the pore fluid, p is the fluid pressure, z is the vertical distance (positive downwards), ρ is the density of the pore fluid, and g is the acceleration due to gravity. Equation A1 is analogous to the steady-state equation for one-dimensional heat conduction (Carslaw and Jaeger, 1959), pressure taking the place of temperature.

If the Darcy velocity, density, viscosity, and permeability are all invariant with depth, equation A1 integrates to:

$$p = \rho g z - (q\mu/k)z \tag{A2}$$

This is the equation of a straight line (Fig. 2A). It is analogous to a linear thermal gradient in the Earth's crust (Carslaw and Jaeger, 1959). In equation A2, the first term on the right represents a hydrostatic gradient, and the second term represents an overpressure gradient. For example, in equation A1, take $(dp/dz - \rho g) = 2 \times 10^{3}$ Pa m^{-1}. If the fluid viscosity is $\mu = 10^{-3}$ Pa s (the viscosity of water) and the intrinsic permeability is $k = 10^{-17}$ m^{2} (10^{-5} darcy), the Darcy velocity will be $q = 2 \times 10^{-11}$ m s^{-1} (about 0.6 mm/a).

If there is a jump in permeability, for example from layer A to layer B, the pressure gradient also jumps. However, the Darcy velocity must be identical in both layers. Therefore from equation A1 the ratio of pressure gradients in layers A and B is equal to the inverse ratio of their permeability values:

$$(dp/dz)_A/(dp/dz)_B = k_B/k_A \tag{A3}$$

This implies that a pressure ramp will occur in a layer of small permeability. For example, take the same values as before for the overpressure gradient, the fluid viscosity, the intrinsic permeability of an overburden, and the Darcy velocity, but insert a sealing layer, 13 times less permeable (Fig. 2B). The pressure then ramps to a lithostatic value at the base of the sealing layer.

Now consider the additional possibility that some fluid generates (or vanishes) within the material. The vertical velocity therefore varies with depth:

$$dq/dz = - Q \qquad \text{(A4)}$$

Here Q represents a source (or sink). It measures a rate of increase (or decrease) in volume, per unit initial volume.

On deriving equation A1 with respect to z and substituting equation A4, we obtain:

$$d^2p/dz^2 = Q\mu/k \qquad \text{(A5)}$$

If the source term is invariant with depth, equation A5 integrates to:

$$dp/dz = \rho g - q\mu/k + (Q\mu/2k)z \qquad \text{(A6)}$$

Here equation A1 has provided the constant of integration.

Finally, if all parameters except the pressure are constant, equation A6 integrates to:

$$p = \rho gz - (q\mu/k)z + (Q\mu/2k)z^2 \qquad \text{(A7)}$$

This is the equation of a parabola (Fig. 2C). It is analogous to the equation for production and flow of heat in the Earth's crust (Carslaw and Jaeger, 1959). In equation (A7), the source and the permeability both contribute to a quadratic term in z and their ratio determines the sharpness of the resulting pressure peak. For example, take the same values as before for the fluid viscosity, and for the overpressure gradient, intrinsic permeability, and Darcy velocity in the overburden. Now assume that the fluid comes from an underlying source layer, which is 2 km thick and 40 times less permeable than the overburden (Fig. 2C). From equation A7, the rate of fluid generation in the source layer will be $Q = 2 \times 10^{-14}\ s^{-1}$. If the upper half of the source layer accounts for upward flow through the overburden, and the lower half accounts for downward flow through the substrate, which is taken to be a sink, then the fluid pressure reaches a lithostatic value about half way up the source layer.

References

Byerlee, JD (1978) Friction of Rock. *Pageophysics*, **116**, 615-626.

Carslaw HS & Jaeger JC (1959) *Conduction of heat in solids*. 2nd edn. Clarendon Press, Oxford, 510 pp.

Cobbold PR, Durand S, Mourgues R, (2001) Sandbox modelling of thrust wedges with fluid-assisted detachments. *Tectonophysics*, **334**, 245-258.

Cosgrove JW (1995) The expression of hydraulic fracturing in rocks and sediments. In: *Fractography: fracture tomography as a tool in fracture mechanics and stress analysis* (ed. M.S. Ameen) Geological Society of London Special Publication, **92**, 187-196.

Cosgrove JW (2001) Hydraulic fracturing during the formation and deformation of a basin: a factor in the dewatering of low-permeability sediments. *American Association of Petroleum Geologists Bulletin*, **85**, 737-748.

Durney DW & Ramsay JG (1973) Incremental strains measured by syntectonic crystal growths. In*: Gravity and tectonics* (ed. by K. A. De Jong & R. Scholten), Wiley, New York, pp. 67-96.

Galland O, Cobbold PR, Hallot E, de Bremond d'Ars J & Delavaud G (2006) Use of vegetable oil and silica powder for scale modelling of magmatic intrusion in a deforming brittle crust. *Earth and Planetary Science Letters*, **243**, 786-804.

Hilgers C & Urai JL (2002) Experimental study of syntaxial vein growth during lateral fluid flow in transmitted light: first results. *Journal of Structural Geology*, **24**, 1029-1043.

Hilgers C & Urai JL (2005) On the arrangement of solid inclusions in fibrous veins and the role of the crack-seal mechanism. *Journal of Structural Geology*, **27**, 481-494.

Hillier RD & Cosgrove JW (2002) Core and seismic observations of overpressure-related deformation within Eocene sediments of the Outer Moray Firth, UKCS. *Petroleum Geoscience*, **8**, 141-149.

Hillis RR (2003) Pore pressure/stress coupling and its implications for rock failure. In: *Subsurface sediment mobilization* (eds Van Rensbergen P, Hillis RR, Maltan AJ & Morley CK) Geological Society of London Special Publication, **216**, 359-368.

Hubbert MK & Rubey WW (1959) Role of fluid pressure in mechanics of overthrust faulting. 1. Mechanics of fluid-filled porous solids and its application to overthrust faulting. *Geological Society of America Bulletin*, **70**, 115-166.

Hubbert MK & Willis DG (1957) Mechanics of hydraulic fracturing. *Petroleum Transactions of the American Institute of Mining Engineers*, **210**, 153-168.

Jaeger JC & Cook NGW (1979) *Fundamentals of rock mechanics.* 3rd edn, Chapman and Hall, London, 593 pp.

Lang WD, Spath LF & Richardson WA (1923) Shales-With-'Beef', a sequence in the Lower Lias of the Dorset Coast. *Quarterly Journal of the Geological Society,* **79**, 47-99.

Lash GG & Engelder T (2005) An analysis of horizontal microcracking during catagenesis: Example from the Catskill delta complex. *American Association of Petroleum Geologists Bulletin*, **89**, 1433-1449.

Mandl G & Harkness RM (1987) Hydrocarbon migration by hydraulic fracturing. In: *Deformation of sediments and sedimentary rocks* (eds Jones ME & Preston RMF), Geological Society of London Special Publication, **29**, 39-53.

Means WD & Li T (2001) A laboratory simulation of fibrous veins: some first observations. *Journal of Structural Geology*, **23**, 857-863.

Mourgues R & Cobbold PR (2003) Some tectonic consequences of fluid overpressures and seepage forces as demonstrated by sandbox modelling. *Tectonophysics*, **376**, 75-97.

Nichols RJ, Sparks RSJ & Wilson CJN (1994) Experimental studies of the fluidization of layered sediments and the formation of fluid escape structures. *Sedimentology*, **41**, 233-253.

Nollet S, Hilgers C & Urai J (2006) Experimental study of polycrystal growth from an advecting supersaturated fluid in a model fracture. *Geofluids*, **6**, 185-200.

Parnell J (1999) Petrographic evidence for emplacement of carbon into Witwatersrand conglomerates under high fluid pressure. *Journal of Sedimentary Research*, **69**, 164-170.

Parnell J & Carey PF (1995) Emplacement of bitumen (asphaltite) veins in the Neuquén Basin, Argentina. *American Association of Petroleum Geologists Bulletin*, **79**, 1798-1816.

Parnell J, Honghan C, Middleton D, Haggan T & Carey P (2000) Significance of fibrous mineral veins in hydrocarbon migration: fluid inclusion studies. *Journal of Geochemical Exploration*, **69-70**, 623-627.

Price NJ & Cosgrove JW (1990) *Analysis of geological structures*. Cambridge University Press, 502 pp.

Ramsay JG (1980) The crack-seal mechanism of rock deformation. *Nature*, **284**, 135-139.

Shearman DJ, Mossop G, Dunsmore H & Martin M (1972) Origin of gypsum veins by hydraulic fracture. *Transactions of the Institute of Mining and Metallurgy*, **B181**, 149-155.

Sibson RH (2003) Brittle-failure controls on maximum sustainable overpressure in different tectonic regimes. *American Association of Petroleum Geologists Bulletin*, **87**, 901-908.

Sorby HC (1860) On the origin of " cone-in-cone ". British Association for the Advancement of Science, Report of the 29th Meeting, 1859, Transactions of Sections, Geology, p. 124.

Stoneley R (1983) Fibrous calcite veins, overpressures, and primary oil migration. *American Association of Petroleum Geologists Bulletin*, **67**, 1427-1428.

Swarbrick RE, Osborne MJ & Yardley GS (2002) Comparison of overpressure magnitude resulting from the main generating mechanisms. In*: Pressure regimes in sedimentary basins and their prediction* (eds by A.R. Huffman & G.L. Bowers), American Association of Petroleum Geologists Memoir, **76**, 1-12.

Taber S (1918) The origin of veinlets in the Silurian and Devonian strata of New York. *Journal of Geology*, **26**, 56-63.

Underhill JR & Stoneley R (1998) Introduction to the development, evolution and petroleum geology of the Wessex Basin. In*: Development, evolution and petroleum geology of the Wessex Basin* (ed. Underhill JR), Geological Society of London Special Publication, **133**, 1-18.

Valverde JM, Ramos A, Castellanos A & Watson PK (1998) The tensile strength of cohesive powders and its relationship to consolidation, free volume and cohesivity. Powder *Technology*, **97**, 237-245.

Von Terzaghi K (1923) Die Berechnung der Durchlässigkeitsziffer des Tones aus dem Verlauf der hydrodynamischen Spannungerscheinungen. Sitzungsberichte der Akademie der Wissenschaften in Wien, mathematischnaturwissenschaftliche Klasse, Abteilung IIa, **132**, 125-138.

Watson PK, Valverde JM & Castellanos A (2001) The tensile strength and free volume of cohesive powders compressed by gas flow. *Powder Technology*, **115**, 45-50.

Wiltschko DV & Morse JW (2001) Crystalization pressure versus “crack seal” as the mechanism for banded veins. *Geology*, **29 (1)**, 79-82.

Figure captions

Fig. 1. A. White veins of fibrous calcite ("beef") within black shale of the "Shales-with-Beef", Lyme Regis, Dorset Coast, SW England. B. Nested cones of fibrous calcite ("cone-in-cone") from same locality.

Fig. 2. Theoretical profiles of fluid overpressure due to Darcy flow. For equations and parameters used in calculations, see Appendix.

A. Linear profile due to uniform upward flow through medium of uniform permeability. Fluid comes from below. Its pressure gradient is greater than hydrostatic, but smaller than lithostatic. B. Pressure ramp due to uniform upward flow through sealing layer. Fluid comes from below. Pressure reaches lithostatic value at base of seal. C. Parabolic hump due to fluid generation within source layer. No fluid comes from below. Pressure reaches lithostatic value about half way up source layer.

Fig. 3. Horizontal hydraulic fractures due to upward fluid flow and resulting seepage forces in pack of powdered silica. Container is cylinder of transparent plastic. Horizontal fractures connect to vertical channels near upper surface of powder.

Fig. 4. Idealized vertical section through homogeneous column of rock, containing horizontal fracture. Acting on each element of solid framework are force of gravity, F_g, and seepage force, F_s. Sides of column are stationary, rigid and frictionless.

Fig. 5. Mohr circle for stress and linear Coulomb failure envelope for non-cohesive material.

Fig. 6. Mohr circles and envelopes for elastic behaviour or for yield, assuming a minimum stress of 100 MPa.

Fig. 7. Reduction in state of effective stress due to overpressure, *P*. Mohr circle shifts to left by an amount equal to *P*.

Fig. 8. Influence of increasing overpressure on position and size of Mohr circle for effective stress (after Mourgues and Cobbold, 2003).

Fig. 9. Influence of fluid overpressure in a material that has true tensile strength. As overpressure increases, Mohr circles for effective stress become progressively smaller in compressive field, then larger again in tensile field. Mohr circle may touch failure envelope at point on horizontal axis. Least principal effective stress is then tensile and vertical, and failure results in horizontal fracture.

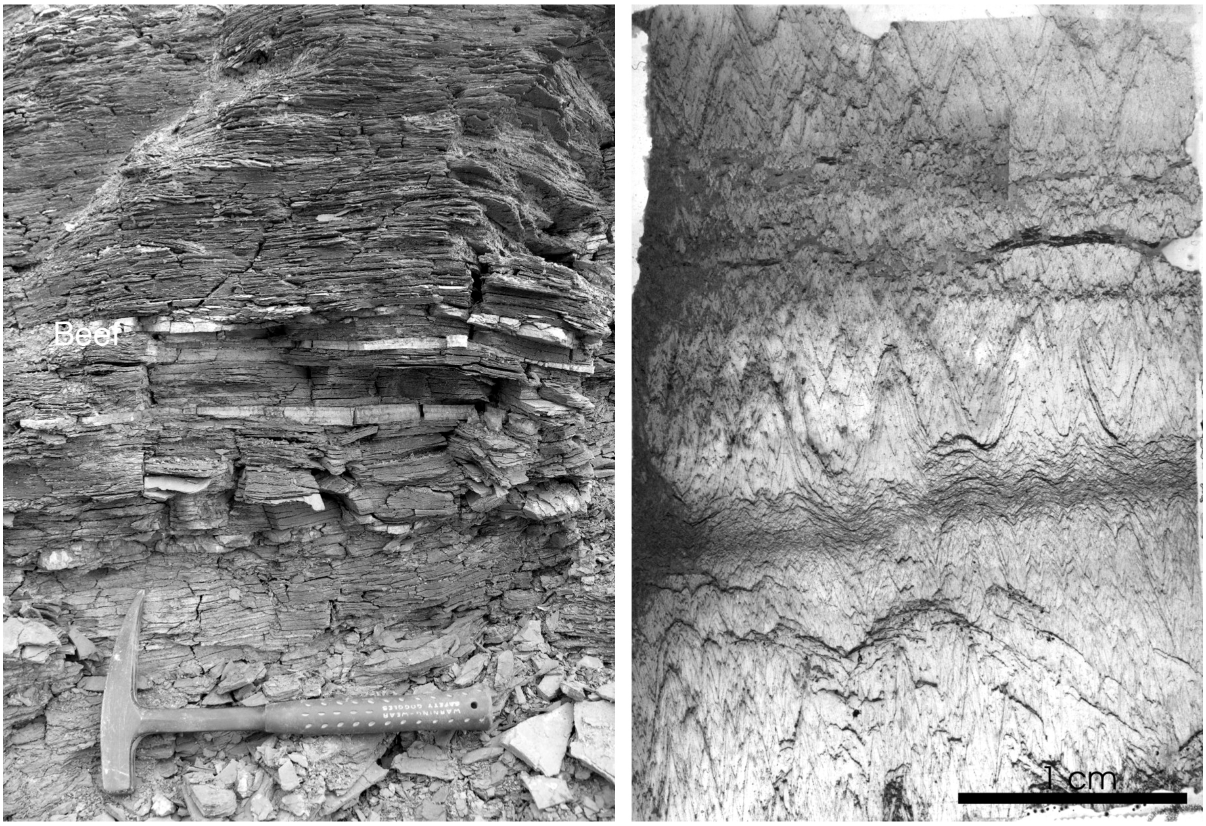

Figure 1

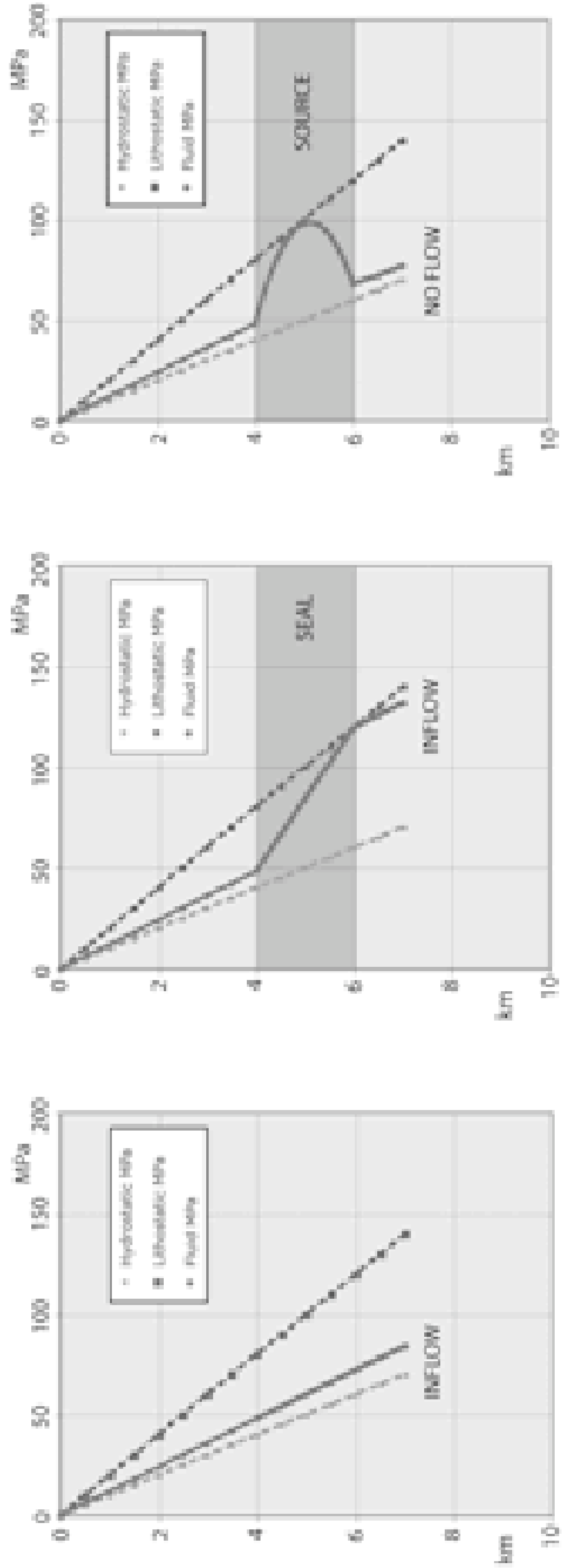

Figure 2

631 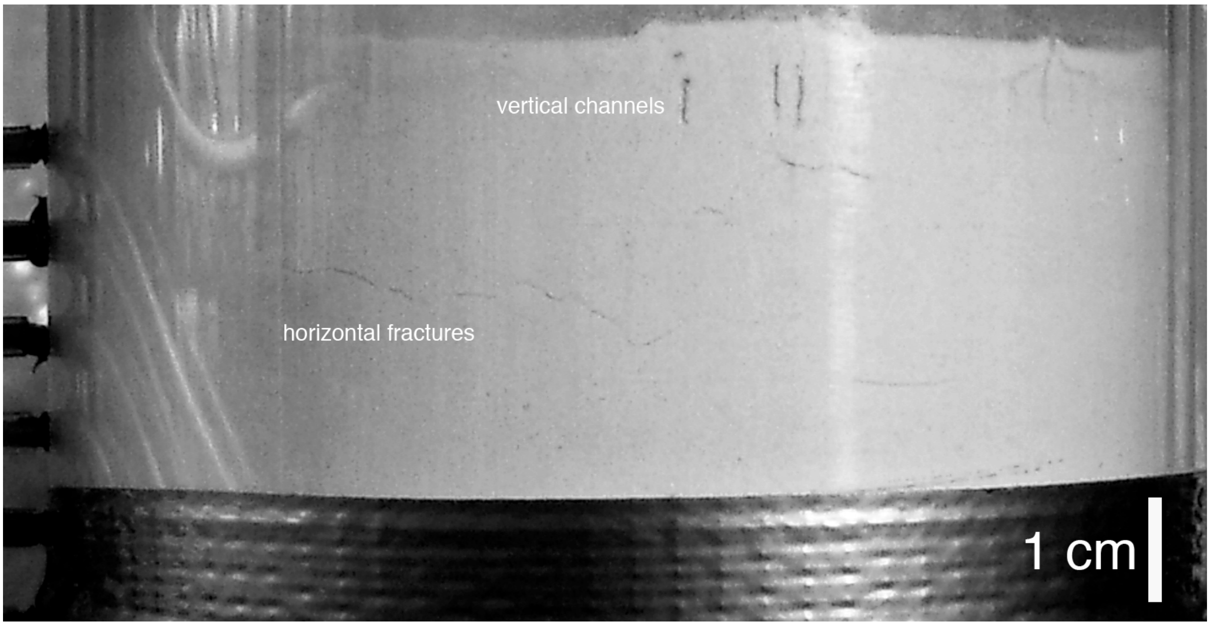

632

633

634

635

636

637 Figure 3

638

639

640

641

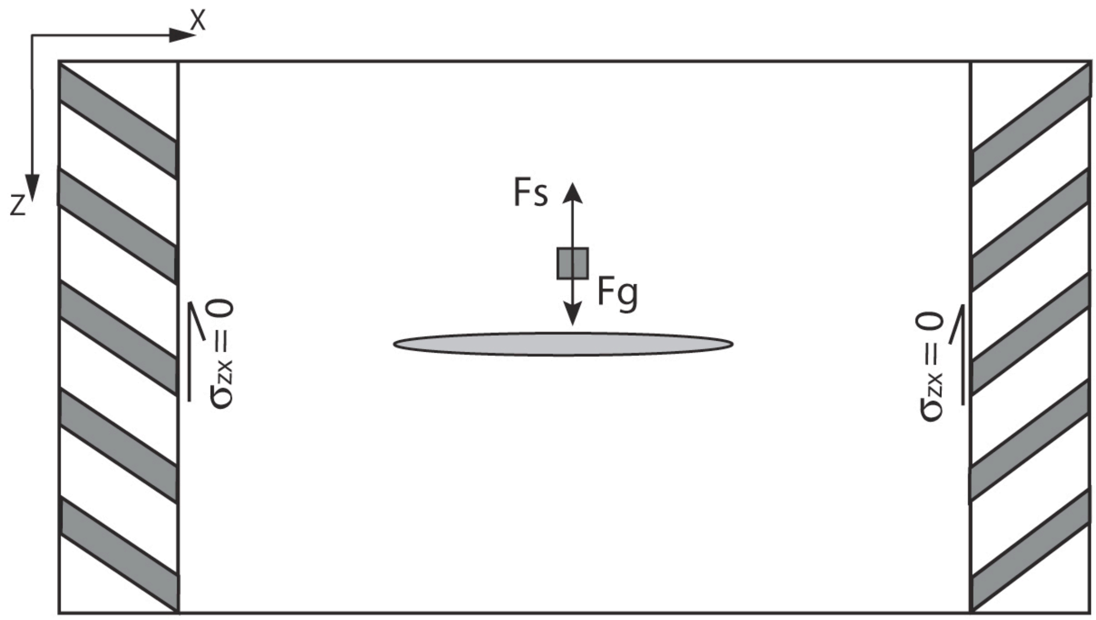

Figure 4

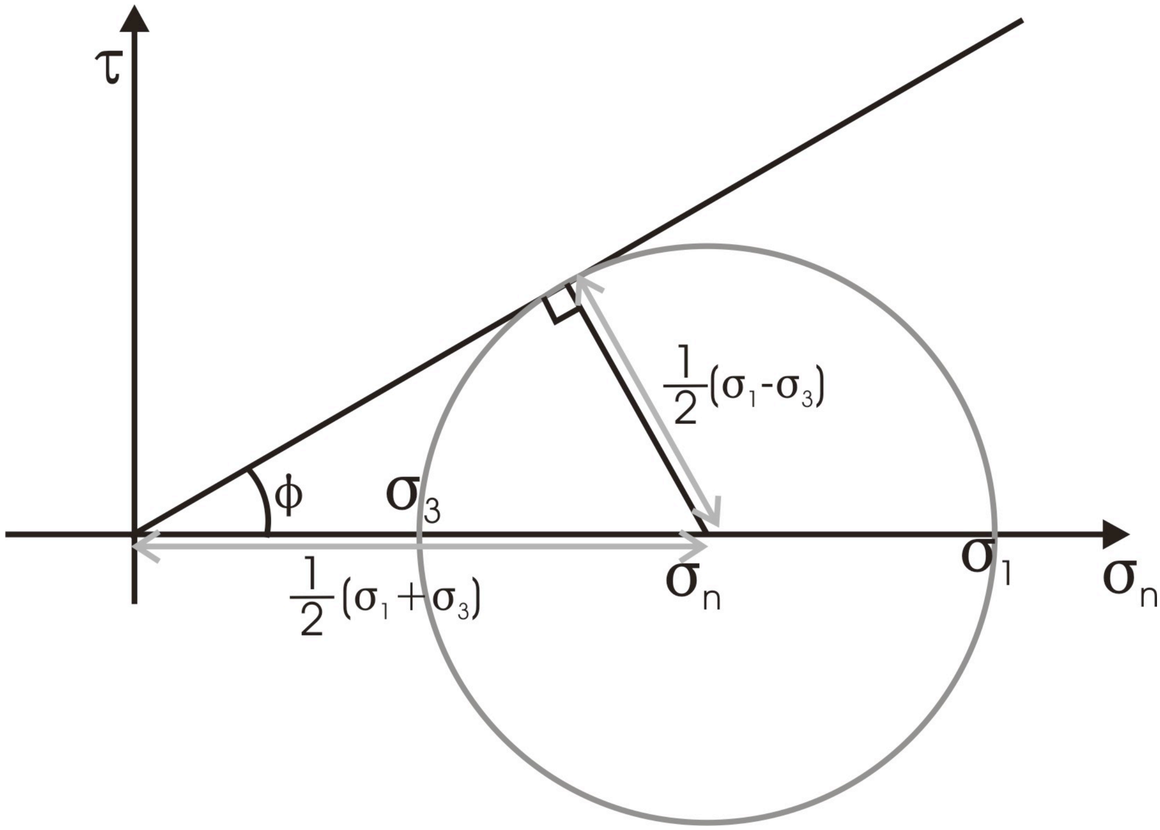

Figure 5

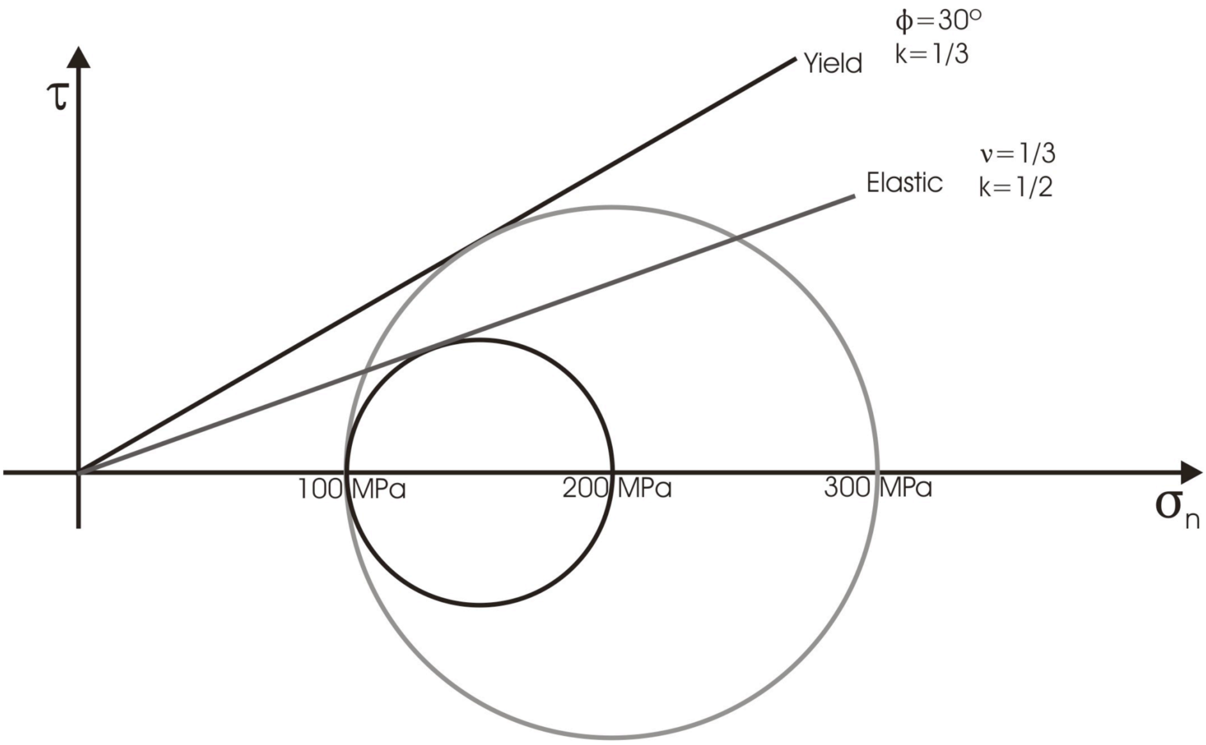

Figure 6

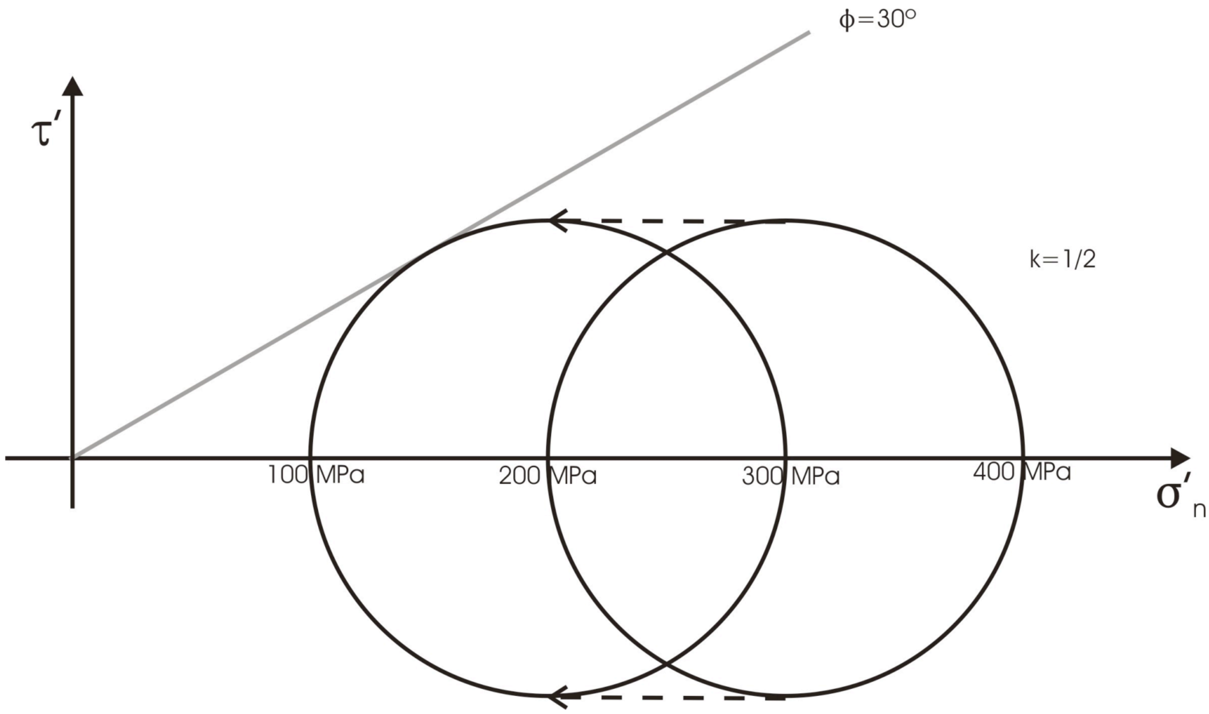

Figure 7

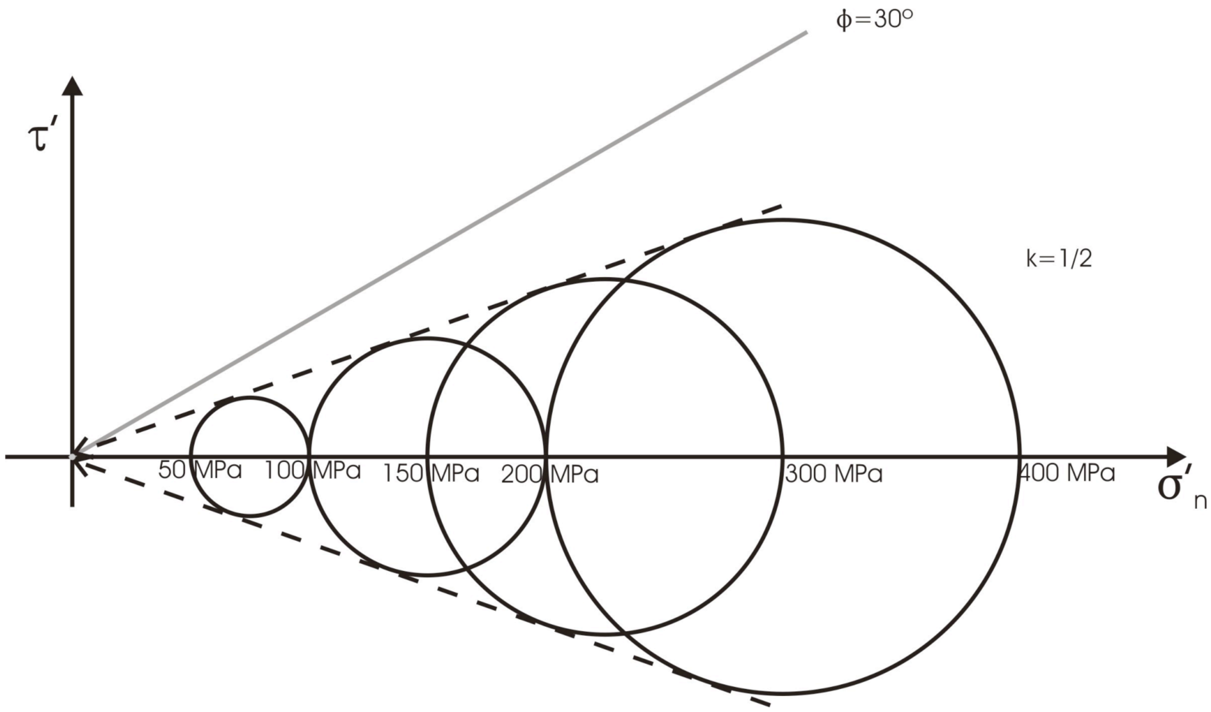

Figure 8

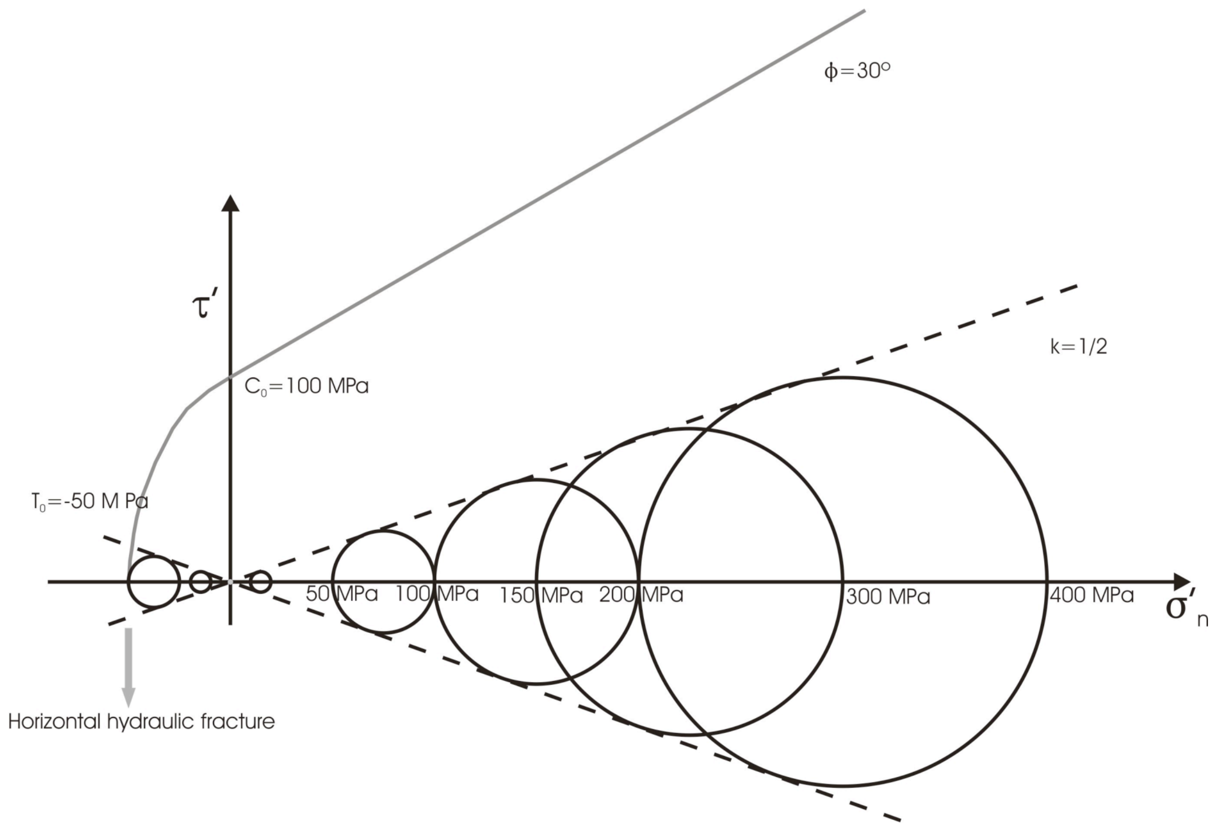
ϕ=30°
τ′
k=1/2
C_0=100 MPa
T_0=-50 M Pa
50 MPa
100 MPa
150 MPa
200 MPa
300 MPa
400 MPa
σ′n
Horizontal hydraulic fracture

Figure 9